Experimental Demonstration of Extended 5G Digital Fronthaul over a Partially-Disaggregated WDM/SDM Network

J. M. Fabrega, *Senior Member, IEEE,* R. Muñoz, *Senior Member, IEEE,* L. Nadal, *Senior Member, IEEE,* C. Manso, M. Svaluto Moreolo, *Senior Member, IEEE,* R. Vilalta, *Senior Member, IEEE,* R. Martínez, *Senior Member, IEEE,* F. J. Vílchez D. Pérez Galacho, S. Sales, *Senior Member, IEEE,* E. Grivas, J. P. Turkiewicz, S. Rommel, and I. Tafur Monroy

***Abstract*—We demonstrate experimentally a 5G digital fronthaul network that relies on multi-adaptive bandwidth/bitrate variable transceivers (BVTs) and an autonomic software-defined networking (SDN) control system for partially-disaggregated wavelength division multiplexing (WDM)/space division multiplexing (SDM) . Transmission of 256-QAM 760.32 MHz orthogonal frequency-division multiplexing (OFDM) radio signal is performed, with a total radio transmission capacity of 5.667 Gb/s. Digitized signal samples are carried as a 22.25 Gb/s digitized radio-over-fiber (DRoF) data stream and transmitted over a WDM/ SDM infrastructure including 40-wavelength 100-GHz arrayed waveguide gratings (AWGs) and 19-core fiber. The autonomic SDN controller deploys a control loop for the multi-adaptive OFDM-based BVTs that monitors the per-subcarrier signal to noise ratio (SNR) and computes the optimal constellation based on the actual signal degradation. error vector magnitude (EVM) below the target 2.1% was achieved.**

***Index Terms*—Fronthaul, Optical Networks, Optical transmission, SDM, 5G, SDN.**

I. Introduction

IN traditional radio access networks (RANs), the baseband unit (BBU) , where the radio signal processing takes place, is co-located with the remote radio units (RRUs) at the base station. The transport network supporting the interface between the BBUs and the mobile core network is called the mobile backhaul. It has relaxed requirements for latency and capacity, and traditionally is deployed in packet-based network (e.g., Ethernet, IP/MPLS). The current trend in mobile networks is to evolve towards a centralized radio access network (C-RAN) architecture, where the BBUs are decoupled from the RRUs and moved far away to a central office (CO) [1]. The key benefits of C-RAN approach are the cost reduction, e.g. due to the infrastructure scale effects as well as sophisticated signal processing and control functions [2]. The transport network connecting the RRUs and BBUs is called a mobile fronthaul network. Such network is usually implemented by means of the so-called DRoF, transporting the digitized radio waveform from the RRU to the BBU and vice versa. DRoF requires a high capacity and low latency network [3]. The most popular standard for DRoF in 4G networks is the common public radio interface (CPRI) [4], with the packet variant of eCPRI.

The DRoF fronthaul can be deployed using different transmission technologies [5]. The most popular is to deploy point-to-point WDM links with dedicated fiber. Another approach is to relay on optical access technologies such as NG-PON2, WDM-P2P, XGS-PON [6]. These solutions have limited dynamic reconfigurability. Also, they operate with the fixed wavelengths and bitrates as well as offer limited transmission capacity.

For 5G, 3GPP specifies the radio signals able to deliver capacities beyond 1 Gbit/s per user [7]. Since bandwidth and constellation size are increased, the DRoF fronthaul network requires a significantly larger capacity. Traffic estimations for DRoF show that several hundreds of Gbit/s, and even Tbit/s will be needed per antenna site [8].

This need can be addressed by upgrading the fiber network with multi-core fibers (MCFs) in order to realize SDM [9], [10]. In fact, the use of MCFs is the straightforward solution for scaling up capacity in a cost effective way [11]. By combining WDM and SDM, the total capacity of the fronthaul network can be substantially increased, enabling to setup specific WDM/SDM channels according to the service requirements [12].

In terms of network development, the telecom operators are looking at the optical network disaggregation approach because it entails cost-reduction, while enabling the migration and upgrade of network components avoiding vendor lock-in [13]. In fact, two optical disaggregation models can be considered: partially or fully disaggregated. In the first model, the transponders are provided by multiple vendors with open application programming interfaces (APIs) to interface with

Work supported by the EC H2020 BLUESPACE (762055) and Spanish MICINN AURORAS (RTI2018-099178) projects.

J. M. Fabrega, R. Muñoz, L. Nadal, C. Manso, M. Svaluto Moreolo, R. Vilalta, R. Martínez and F. J. Vílchez are with the Optical Networks and Systems Department of the Centre Tecnològic de Telecomunicacions de Catalunya (CTTC/CERCA), Castelldefels, Spain, e-mail: jmfabrega@cttc.es, rmunoz@cttc.es, lnadal@cttc.es, cmanso@cttc.es, msvaluto@cttc.es, rvilalta@cttc.es, rmartinez@cttc.es, jvilchez@cttc.es

D. Pérez Galacho and S. Sales are with the ITEAM institute, Universitat Politècnica de València, Valencia, Spain, e-mail: diepega@iteam.upv.es, ssales@iteam.upv.es

E. Grivas is with Eulambia Advanced Technologies Ltd., Athens, Greece, e-mail: egrivas@eulambia.com

J. P. Turkiewicz is with Orange Polska, Warsaw, Poland, e-mail: Jaroslaw.Turkiewicz@orange.com

S. Rommel and I. Tafur Monroy are with the Institute for Photonic Integration, Eindhoven University of Technology, Eindhoven, Netherlands, e-mail: s.rommel@tue.nl, i.tafur.monroy@tue.nl

Manuscript received July 15th, 2020; revised YYYY; published ZZZZZ.

the transport SDN controller, whilst the remaining elements, known as the optical line system (OLS), remain as a single-vendor infrastructure [13]. The OLS controller is provided by its vendor with open APIs to interface with the transport SDN controller. In the second model, all optical network elements can be provided by different vendors with standard APIs to the transport SDN controller. Each of these elements has a unified data modelling and open APIs to the SDN control system.

In this paper, we experimentally demonstrate a DRoF approach that uses WDM/SDM in combination with an agile data plane and advanced control plane. Our approach also aims at integrating the optical access and metro networks, both at the transport and control level, thanks to the deployed SDM/WDM. The same CO can be shared by different optical access networks that are connected through an optical metro network. In this scenario, the latency induced in the mobile fronthaul needs to be controlled to be lower than 20 ms [14]. From the data plane perspective, the key elements are the so-called BVTs [15], [16]. In fact, the BVTs implement a range of advanced functionalities, such as different bit rates and a dynamic variation and adaptation of modulation format and symbol rate. In this regard, optical OFDM is a promising candidate thanks to its superior granularity and capabilities for transmission reconfiguration [17]. Moreover, in this paper, we also extend the autonomic SDN control architecture proposed in [18] for partially-disaggregated optical networks, since it can be regarded as the first step when moving towards a fully disaggregated network [13]. To this end, the configuration and monitoring of the integrated access/metro optical network acting as the mobile fronthaul is delegated to a dedicated OLS controller. Then, the SDN controller interfaces with the OLS controller and the transceiver agents in order to provide end-to-end fronthaul transport services involving both the access/metro optical network and the BVTs.

The paper is structured as follows. In section II the proposed network scenario is detailed and discussed, providing the details of the data plane and the SDN control system. Section III, deals with the experimental setup, whereas section IV reports the results. Finally, conclusions are drawn in section V.

II. Concept and scenario

The considered disaggregated SDM/WDM fronthaul network with OFDM-based BVTs is shown in Fig. 1. Data and control plane aspects of the network are detailed in the following subsections.

A. Network architecture and systems

The network is composed of COs interconnected through an optical aggregation/metro network deployed with, for example, reconfigurable add-drop multiplexers (ROADMs). The COs serve different cell sites (CSs) through an optical distribution network. At the CO, an optical switch provides connectivity between the ROADMs, the optical distribution network used in the access, and optionally a pool of BBUs attached to an array of OFDM-based BVTs [19]. It is worth to mention that not all COs are required to be equipped with a pool of BBUs and BVTs, as shown in Fig. 1. On the access side, the optical switch provides connectivity to either the fan-in/out for SDM transmission [20] or to one or eventually a pool of AWGs or wavelength selective switches (WSSs) for WDM transmission. The CO delivers its data signals to an optical distribution network, whose feeder stage is a MCF that connects the CO with a remote node (RN). At the RN, signals are spatially demultiplexed by means of another fan-in/out device. After the RN, different drop stages are envisioned, either featuring 1-core standard single-mode fiber (SSMF) bundles for continuing SDM scheme or just an SSMF with WDM stages. Finally, the CSs also contain BVTs connected to the RRU and eventual wavelength demultiplexing stages. The RNs are intended as a main space division demultiplexing point and to eventually serve a macro-cell. The CSs are proposed for a small cell service, using SSMF or a bundle of them for the last mile fronthaul. It should be noted that MCFs may show certain core-to-core crosstalk with the corresponding impact on the signal performance. Therefore, we need a control system that is able to react to such signal degradation by interacting with the BVTs.

TABLE I
Extended 5G-NR radio parameters for BBU/RRU.

Parameter	Value
Subcarrier spacing	240 kHz
Num. of points for FFT	4096
Sampling frequency (fs)	983.04 MHz
Number of subcarriers	3168
Constellation	16QAM, 64QAM, 256QAM

The BVTs are programmable transceivers with enhanced capabilities. In our case, we consider OFDM-based BVTs that feature a broad range of parameters to be configured: maximum and minimum capacity (5-50 Gb/s); modulation (OFDM); number of subcarriers (512); bit per symbol / modulation order (BPSK, QAM4, QAM8, QAM16, QAM32, QAM64, QAM128, QAM256); nominal central frequency range (191.494 THz - 195.256 THz); bandwidth (25 GHz); forward error correction (FEC) (hard-decision or soft-decision); and equalization (zero-forcing or minimum mean square error (MMSE)). The parameters able to be configured at the BVT are: status (active, off, standby), frequency slot (nominal central frequency and frequency slot width), FEC , equalization , and constellation. Constellation is set in a per subcarrier basis by including two magnitudes: the bits per symbol and the normalized power per symbol. Therefore, the capacity can be flexibly set by the SDN controller by using bit and power loading [21] to configure a suitable constellation. Also, the BVT has a couple of monitored parameters; the overall bit error ratio (BER) giving a general view of the connection performance, and the SNR per subcarrier, in order to have an idea of the channel response for driving the adaptive modulation of the OFDM subcarriers.

Other important elements are the digital BBUs and RRUs, whose schemes are depicted in Fig. 2. The BBUs are composed of a radio signal generation stage, where a digital radio signal is generated according to the parameters listed in table I. Even though 5G-NR specifies signals up to 400 MHz, in our case we consider an extension to double the standardized

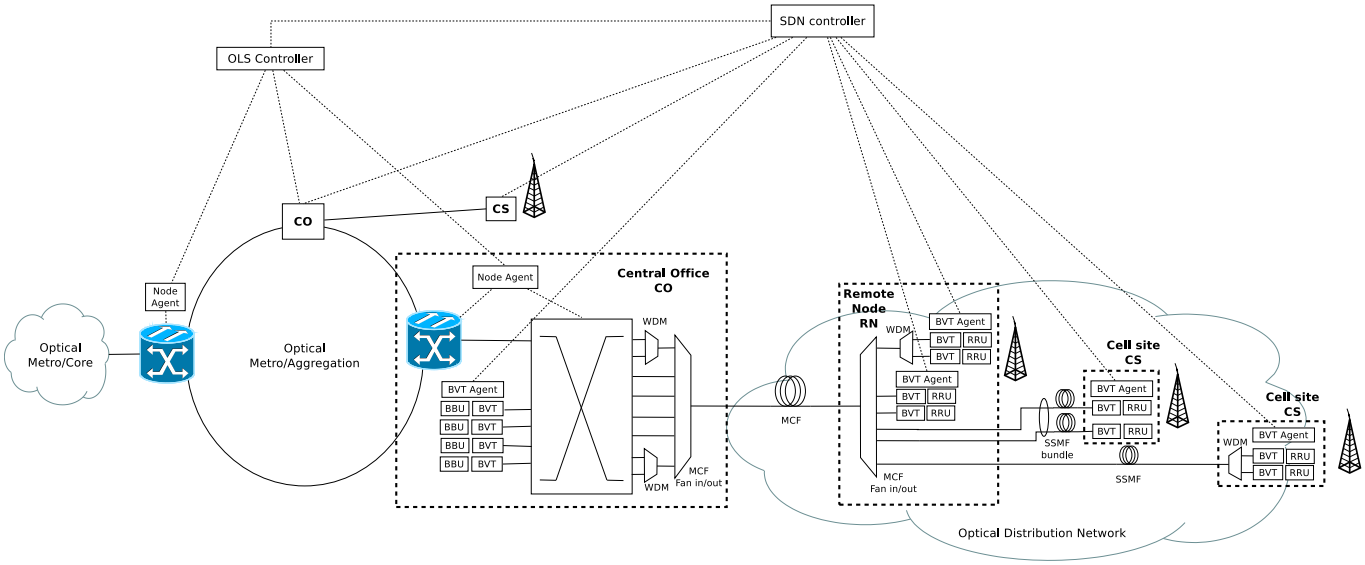

Fig. 1. Example of SDN-controlled partially disaggregated SDM/WDM fronthaul network

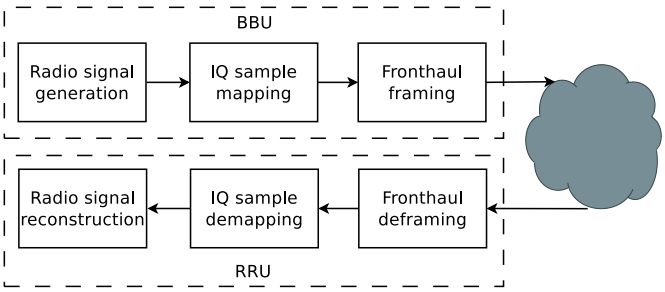

Fig. 2. Internal scheme of BBU and RRU.

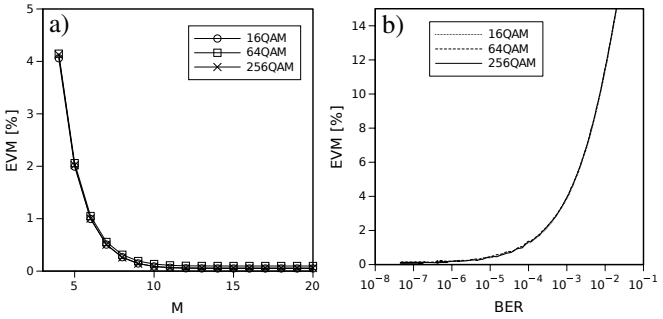

Fig. 3. (a) EVM-floor as a function of the number of bits considered for digitizing. (b) EVM as a function of BER of digitized samples.

bandwidths by combining the maximum subcarrier spacing and maximum number of subcarriers. This signal is then sampled at 983.04 MHz and digitized at M bits per sample, with M ranging between 4 and 20. Please note that the radio signal is clipped at ± 3 times its standard deviation in order to ensure a normalized and unbiased digitization scale. The resulting in-phase and quadrature (I/Q) samples are mapped and framed following the CPRI principles [4]. Every 5120 bits a 344-bit word is included for control and monitoring purposes. These control and monitoring words are simple random bits generated for taking into account the associated overhead. The resulting data is then injected into the corresponding BVT. At the RRU, incoming data from the BVT is deframed, I/Q samples are demapped and the radio signal is reconstructed.

The blocks of Fig. 2 have been implemented as a library in Python. A preliminary evaluation is performed in order to evaluate its performance limits and relationship between the figures of merit of DRoF and analog radio-over-fiber (ARoF). Therefore, an ideal additive white Gaussian noise channel is considered between BBU and RRU blocks. 256 OFDM radio frames are generated and processed accordingly. BER has been computed by error counting at the input of RRU, while EVM has been computed after radio signal detection. Different radio signal constellations have been tested according to table I. Results are shown in Fig. 3. There we observe an EVM floor due to signal clipping and the inherent quantization associated to the signal digitization. As expected, this EVM floor decreases rapidly when increasing the number of bits per sample (M), converging to values around 0.1 % for all the constellations tested. Interestingly, $M = 10$ can be set as the limit to ensure these values.

Regarding target EVM values before the radio wave radiation elements (after power amplifiers), they are of 12.5 % for 16QAM, 8 % for 64QAM and 3.5 % for 256QAM [7]. Since power amplifiers have typical noise figures of 4.5 dB, the targeted EVM at the output of RRU block is expected to be 7.5 % for 16QAM, 4.8 % for 64QAM and 2.1 % for 256QAM. Therefore, in terms of EVM floor limit, the system is compliant with those values for 16QAM and 64QAM, while 256QAM is limited to operate with values of $M > 5$. In terms of BER for the 256QAM case (the most restrictive), we should ensure BER below $2.63 \cdot 10^{-4}$ when considering $M \geq 10$.

B. Autonomic SDN control of multi-adaptive OFDM-based BVTs in partially disaggregated SDM/WDM fronthaul networks

The considered SDN control system architecture relies on an optical SDN controller managing a fronthaul OLS controller as well as the multi-adaptive OFDM-based BVTs through dedicated SDN agents, as depicted in Fig.1. Therefore, we are facing a partially disaggregated network, since the SDN controller interacts with the different BVT agents and an OLS controller that takes care of the remaining network infrastructure. Previously, we presented in [22] an SDN control system architecture for fully disaggregated networks, where the SDN controller was responsible fir configuring all network elements.

The purpose of the BVT agents is to provide a common API to the SDN controller for the configuration and monitoring of the adaptive optical flows. The SDN agent's API defined for the multi-adaptive OFDM-based BVTs is based on yet another next generation (YANG)/network configuration protocol (NETCONF). We have developed a YANG data model for the configuration functionalities (blueSPACE-DRoF-configuration.yang) and another for the supported capabilities (blueSPACE-DRoF-capability.yang). he BVT YANG models are published online on a public repository at [23]. The parameters that define the supported capabilities by the BVT are: maximum and minimum capacity (5-50 Gb/s), modulation (OFDM), number of subcarriers (512), constellations (BPSK, QAM4, QAM8, QAM16, QAM32, QAM64, QAM 128, QAM256), nominal central frequency range (191.494 THz - 195.256 THz), bandwidth (25 GHz), FEC (hard-decision or soft-decision), and equalization (zero-forcing or minimum mean square error). The parameters able to be configured at the BVT are: status (active, off, standby), frequency slot (nominal central frequency and frequency slot width), FEC , equalization , and constellation. Constellation is set in a per subcarrier basis by means of two vectors: one containing the bits per symbol (e.g. from $L = 2$ up to $L = 8$, corresponding to 2^L quadrature amplitude modulation (QAM)), and another one with the normalized power per symbol for each subcarrier. Therefore, the capacity can be set by the SDN controller by generating the suitable constellation. Also, the BVT has a couple of monitored parameters; the overall BER giving a general view of the connection performance, and the SNR per subcarrier, in order to have an idea of the channel response for driving the adaptive modulation of the OFDM subcarriers. The SDN controller can configure and modify the BVT agents with the allocated nominal central frequency slot, constellation, equalization and FEC by sending `NETCONF RPC <edit-config> (create/merge).` On the other hand, the SDN controller can request the capability parameters or the monitoring parameters by sending `NETCONF RPC <get>` messages to the BVT agents.

The OLS controller manages all switching elements and is responsible for providing transport connectivity services between pairs of BVTs across the whole fronthaul network. A detailed description of the considered fronthaul OLS controller architecture for the target WDMSDM network with open interfaces is provided in [24] by the authors. The interface between the SDN controller and the fronthaul OLS controller is based on the transport application programming interface (TAPI) [25]. TAPI defines a common YANG data model for the SDN control plane functions (e.g., path computation, topology and connection provisioning) and uses RESTconf as protocol. The optical SDN controller gets a TAPI context from the fronthaul OLS controller. It is defined by a set of service interface points (SIPs), which enables the optical SDN controller to request connectivity services (e.g. optical channels) between any pair of SIPs. Each SIP defines an endpoint available for connections and its characteristics. Similarly, the optical SDN controller also exposes a TAPI context to its customers, e.g a network function virtualization (NFV) orchestrator.

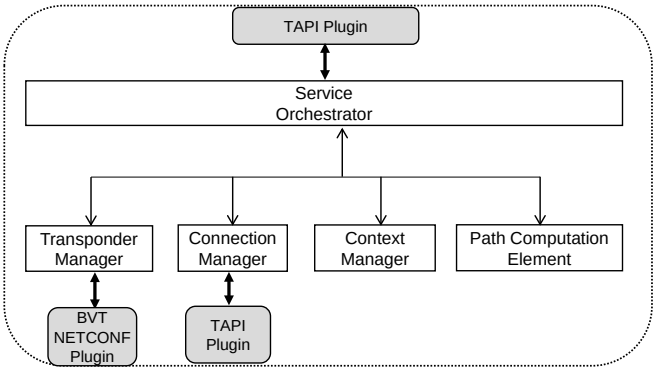

Fig. 4. Optical SDN controller architecture

The considered optical SDN controller architecture is depicted in Fig. 4. It is composed of the following modules:

- Service orchestrator: Processes the incoming TAPI requests from the northbound interface and handles the workflow between the different modules. Also manages connectivity, topology and path computation services.
- Context topology manager: It composes the internal TAPI context topology and serves information from it. The internal TAPI context is composed of the context topology of the fronthaul OLS controller and their SIPs.
- Connection manager: It manages the TAPI connectivity service call and connections in the fronthaul OLS domain. The connection manager can support multiple plugins.
- The path computation element (PCE): It computes a path (nodes/links) between two SIPs based on certain traffic engineering metrics (e.g. unreserved bandwidth).
- Transponder manager: It is responsible for the management of the transponders. It can support multiple plugins, where each plugin is responsible for one type of transopnder. We proposed a specific BVT NETCONF plugin. It is responsible of allocating the required optical bandwidth for the requested capacity, providing the initial configuration parameters of the OFDM-based BVT and processing the monitored per-subcarrier SNR to compute the optimal constellation in a closed-loop by using the Levin-Campello bit/power loading algorithm [21]. The transponder manager can support multiple plugins.

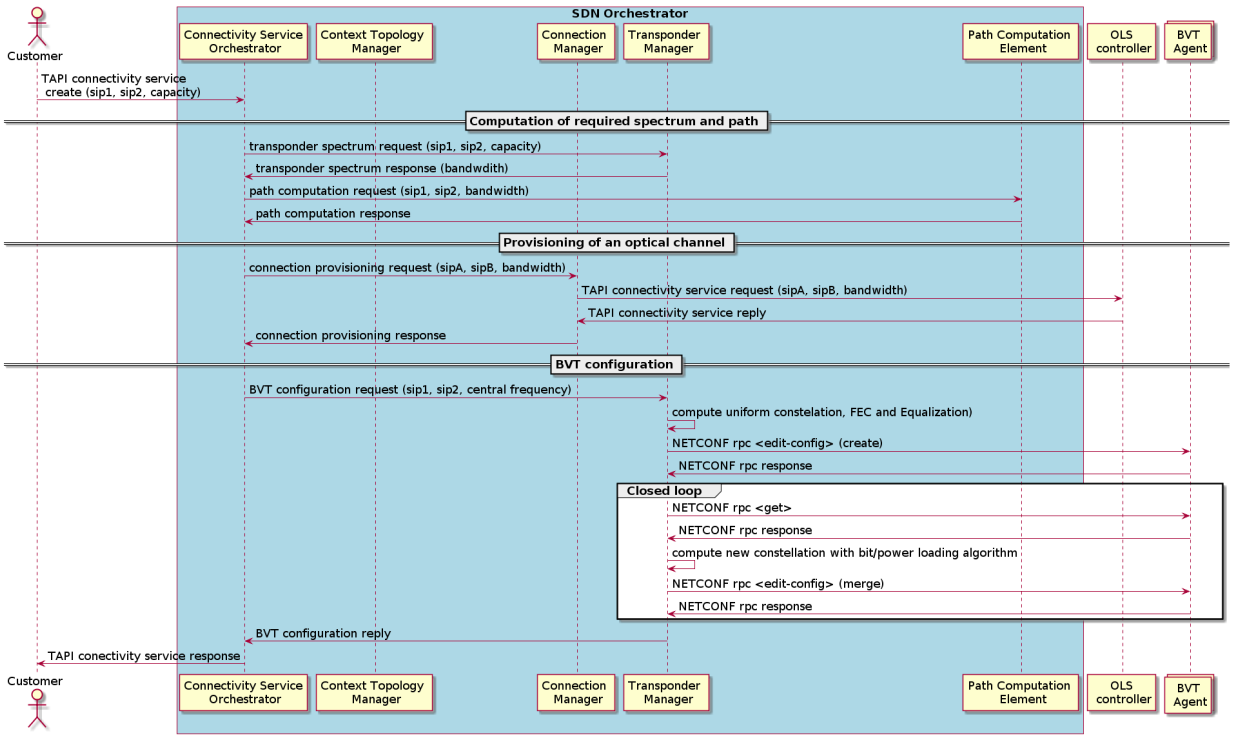

Fig. 5. Autonomic provisioning of a connectivity service with multi-adpative BVTs

The SDN controller provides connectivity services between pairs of OFDM-based BVTs with autonomic reconfiguration of the per-subcarrier constellation based on the monitored SNR. Fig. 5 depicts an example of the workflow involved between the optical SDN controller and the BVT agents for the autonomic provisioning of connectivity services. The provisioning of a connectivity service request between two endpoints is sent to the service orchestrator by means of a TAPI `POST HTTP` request, specifying the two SIPs involved. This process triggers the following actions.

1) Computation of required spectrum and path: After the request is received by the service orchestrator, it requests to the transponder manager the required optical bandwidth (in GHz) from the requested capacity (in Gb/s). Specifically, the transponder manager computes the optical bandwidth from the requested capacity, which is aware of the transceiver supportable capabilities. It considers the worst-case scenario (i.e., without knowledge of the spatial path). Therefore, it computes the required optical bandwidth considering an uniform constellation for all subcarriers with the lower number of bits per symbol, in order to meet the requested capacity. Then, the transponder manager replies with the computed optical bandwidth (e.g., 37.5 GHz) to the service orchestrator.

2) Provisioning of the optical channel: Next, the service orchestrator requests to the PCE the computation of an optical path between the two SIPs. If a feasible path is found, the service orchestrator requests to the connection manager the provisioning of an optical channel with the computed optical bandwidth. Then, the connection manager triggers a TAPI connectivity service call to the fronthaul OLS controller to provision a suitable connection. The OLS is responsible for the assignment of the frequency slot that meets the requested spectrum need.

3) BVT configuration: Once the connection is provisioned, the service orchestrator requests to the transponder manager the configuration of the involved BVTs. The transponder manager specifies the source and destination SIPs, and the nominal central frequency of the frequency slot assigned by the OLS . In order to do that, the transponder manager first allocates the constellation, the equalization and FEC between the source and destination BVTs. It considers again the worst-case scenario (i.e., without knowledge of the channel profile) and allocates an uniform constellation for all subcarriers with the lower number of bits per symbol. Next, the transponder manager configures the nominal central frequency, constellation, equalization and FEC in the BVT. It sends a `NETCONF RPC <edit-config> (create)` message to the BVT agent, and it notifies to the transponder manager if the configuration of the BVT was successful. This operation is performed both for the source BVT (transmitter (Tx)) and the destination BVT (Receiver (Rx)).

4) Closed loop: Once both BVTs are configured successfully, the transponder manager starts a closed loop requests the SNR per sub-carrier at the BVT Rx by sending `NETCONF RPC <get>` messages to the BVT agent. Then, the transpoder manager employs the Levin-Campello bit/power loading algorithm to compute the optimal constellation, including arbitrary sub-carrier suppression to adjust the spectrum of the signal. Finally, the transpoder manager reconfigures the BVTs (Tx and Rx) as performed in the configuration phase, but sending `NETCONF RPC <edit-config> (merge)` messages to

TABLE II
BVT PARAMETERS

BVT #	Nominal central frequency	Duplex
1	Tunable according the case	Adjustable
2	193.3 THz	WDM
3	193.2 THz	WDM
4	Tunable according the case	Adjustable
5	193.3 THz	WDM
6	193.2 THz	WDM
7	193.1 THz	SDM
8	193.1 THz	SDM
9	193.1 THz	SDM
0	193.1 THz	SDM

the BVT agents in order to update the constellation. Once the BVT are reconfigured with the new constellation, the transponder manager notifies to the service orchestrator. Next, the service orchestrator can notify with the TAPI that the connectivity service is provisioned. While the connectivity service is active, the transponder manager is working in a closed loop to continuously monitor the SNR per sub-carrier, apply the bit/power loading algorithm to recompute the constellation, and reconfigure the BVTs if required following the same steps as previously described. Finally, the transponder manager can delete the configuration from the source and destination BVTs by sending the `NETCONF RPC <edit-config> (delete)` messages to the BVT SDN agents when the service orchestrator get a connectivity service delete request.

III. Experimental setup

The experimental setup used for validation is shown in Fig. 6, where a CO is providing connectivity to different RRUs using a passive optical network (PON) infrastructure featuring SDM and WDM. The CO is composed of a BVT pair, a 64×64 optical switching matrix and a 100-GHz AWG. The emulated PON infrastructure is composed by a 25.4-km 19-core MCF feeder segment, and a 2-km SSMF drop segment. In turn, the RN RRUs are composed of a 100-GHz AWG and a BVT pair. This is operated by means of the corresponding BVT agents, an OLS controller, a node agent and an SDN controller.

Since AWGs are used for achieving WDM, a rather fixed set of frequencies is used for the experiment, which are reported in Table III. All the BVTs are configured to employ MMSE-based equalization.

The different BVTs are based on offline processing, hosted in an intermediate computer. Therefore Tx/Rx digital signal processing (DSP) is executed there according to the calls received by the different BVT agents through representational state transfer (REST) API. In this particular setup, the BBUs and RRUs are implemented using off-line processing to handle the bit streams corresponding to 256 OFDM radio frames. Control and monitoring words are randomly generated. 22.25 Gb/s are transmitted, given the parameters mentioned in section II, assuming $M = 10$ bits per sample and including the overheads due to fronthaul CPRI framing (7 %) and optical transmission (6.1 %). This is implemented in the programmable DSP Tx module using Python and Matlab software, which further processes the resulting digital samples to generate another digital OFDM signal (this one for the fronthaul transceiver) according to the constellation specified by the controller. A 4-channel high-speed digital to analog converter (DAC) (up to 64 GSa/s and 13 GHz) is used to convert the digital OFDM signals and provide electrical analog signals that are optically modulated using Mach-Zehnder modulators (MZMs). The MZMs are working at the quadrature point and modulate the light of the C-band tunable lightwave sources (TLSs) managed by the BVT agents.

Each receiver is based on direct detection. An avalanche photo-diode (APD) is emulated by the combination of a gain-stabilized erbium doped fiber amplifier (EDFA), an optical band pass filter and a PIN diode followed by the corresponding transimpedance amplifier. The receiver subsystem is calibrated to obtain -28 dBm sensitivity for a 10^{-3} BER using on-off keying transmission at 10.7 Gb/s. A real-time digital oscilloscope (up to 100 GSa/s and 20 GHz bandwidth) is used as analog to digital converter (ADC). The digital signal is processed offline with the DSP Rx module based on Python software to measure the per-subcarrier SNR and the overall BER.

The fiber network is implemented by using G.652D SSMF and a single feeder of a 25-km 19-core MCF. This feeder fiber has a diameter of 195 μm and a core to core distance of 34 μm. Cores have a diameter of 7.88 μm. A characterization of the fibre including fan-in/out devices is shown in Fig. 7. The average transmission loss is about 10 dB, while core to core crosstalk is below -23.7 dB.

The scheme of the BVT agents implemented to configure and monitor the BVTs is shown in Fig. 8. There, we can see that each agent is composed of a NETCONF server based on Python (pyang [26] and pyangbing [27]) that contains a modular YANG-based data store for the configuration and operational state data. The main element of the BVT agent is the agent core module that is responsible for mapping the high-level actions requested by the NETCONF server into several specific low-level actions on the involved optical sub-systems (i.e., laser and DSP Tx/DAC, and DSP Rx/ADC) by means of the developed function libraries and the corresponding interaction with the computer hosting the DSP modules.

A. Preliminary tests

The cases tested are summarized in table III-A. In order to assess their feasibility from the data plane perspective, a preliminary test is performed for case 1. Results are shown in Fig. 9 in terms of BER and EVM. First a back-to-back (B2B) configuration is evaluated and used as a reference. At -22 dBm, we obtain an EVM of 2.21 % ($2.85 \cdot 10^{-4}$ BER) after RRU processing while at -20 dBm the EVM is 0.6 % ($1.95 \cdot 10^{-5}$ BER) at the same point. Therefore, the 2.1 % EVM received power can be interpolated at -21.9 dBm. Next, the full case 1 (with fibre transmission) is evaluated. In fact, the received power for 2.1 % EVM can be estimated to be -19.0 dBm. Also, we introduce an interfering signal, similar to the one transmitted, over an adjacent core (#7) in order to evaluate crosstalk when measuring EVM and BER at core #1. To obtain the 2.1 % EVM under these circumstances, the

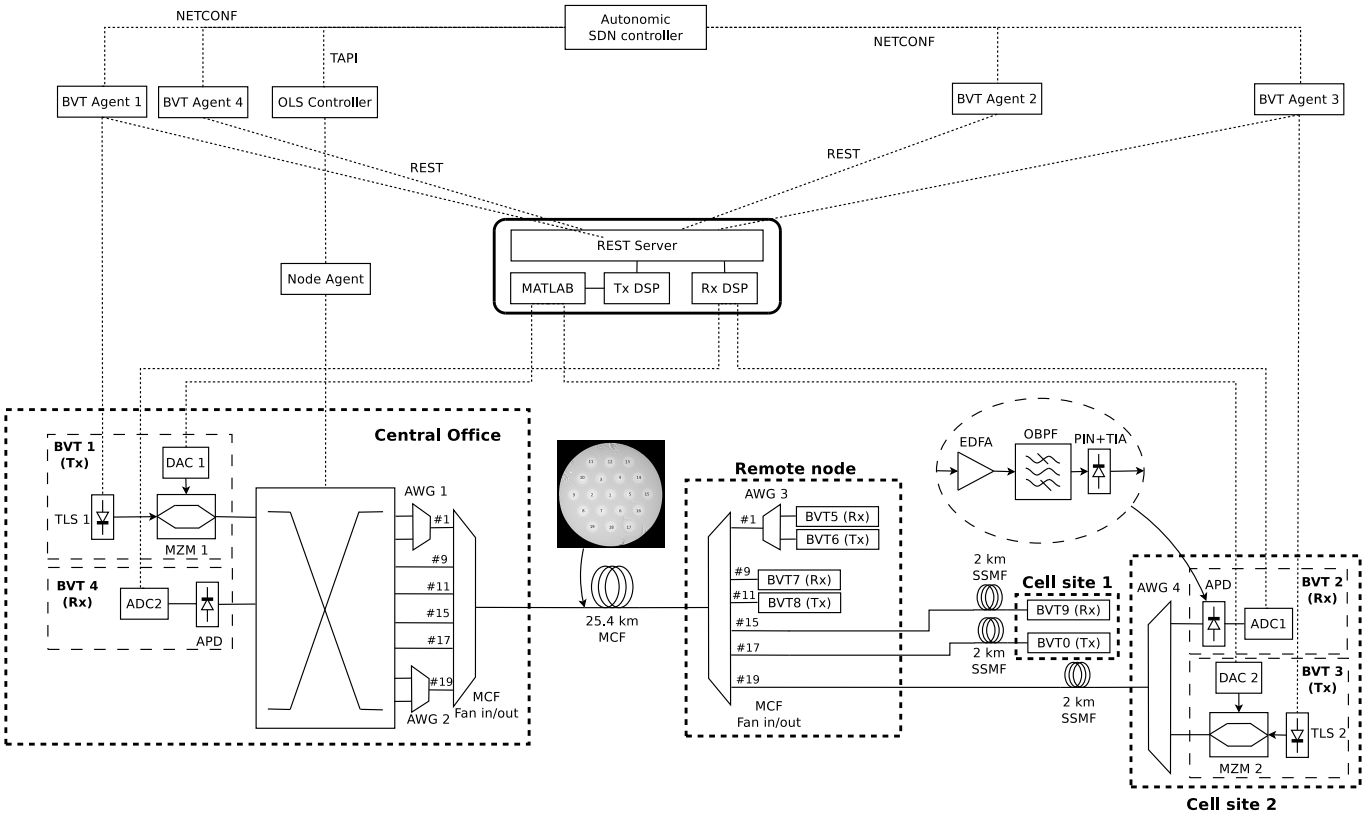

Fig. 6. Experimental setup

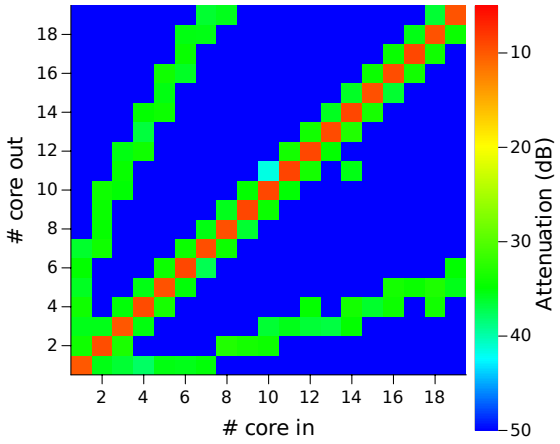

Fig. 7. MCF fiber loss/coupling characterization.

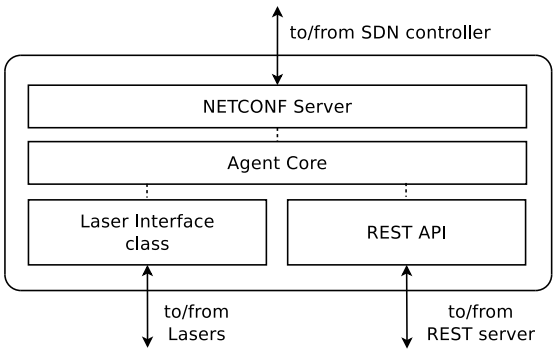

Fig. 8. BVT agent scheme.

TABLE III
CASES TESTED

Case #	Description	BVTs involved
Case 1	CO-RN: WDM duplex	BVT1-BVT5 + BVT6-BVT4
Case 2	CO-RN: SDM duplex	BVT1-BVT7 + BVT8-BVT4
Case 3	CO-CS1: SDM duplex	BVT1-BVT9 + BVT0-BVT4
Case 4	CO-CS2: WDM duplex	BVT1-BVT2 + BVT3-BVT4

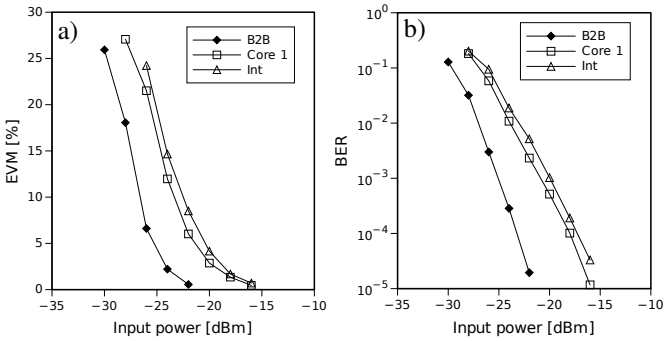

Fig. 9. Results of preliminary test for case 1. EVM (a) and BER (b) as function of the received power.

received power is estimated to be -18.3 dBm, about 0.7 dB worse than in the previous case.

IV. Experimental Results

We have experimentally validated the workflow depicted in Fig. 5, by following a set of the identifiable steps per each

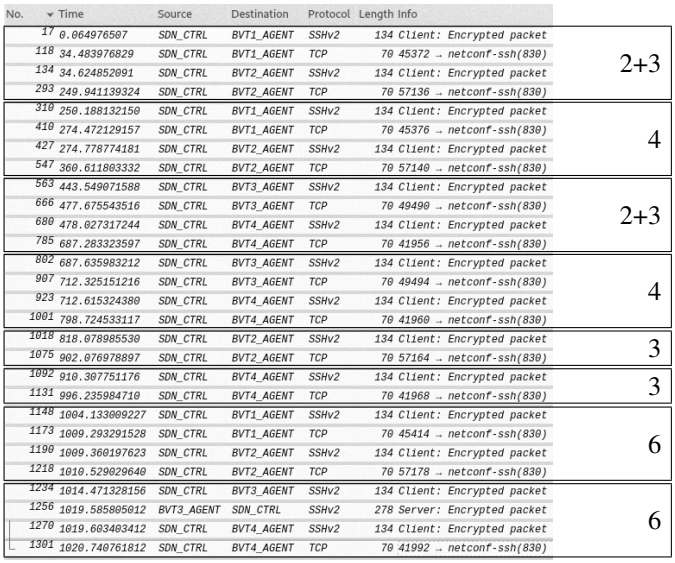

No.	Time	Source	Destination	Protocol	Length	Info	
17	0.064976507	SDN_CTRL	BVT1_AGENT	SSHv2	134	Client: Encrypted packet	2+3
118	34.483976829	SDN_CTRL	BVT1_AGENT	TCP	70	45372 → netconf-ssh(830)	
134	34.624852091	SDN_CTRL	BVT2_AGENT	SSHv2	134	Client: Encrypted packet	
293	249.941139324	SDN_CTRL	BVT2_AGENT	TCP	70	57136 → netconf-ssh(830)	
310	250.188132150	SDN_CTRL	BVT1_AGENT	SSHv2	134	Client: Encrypted packet	4
410	274.472129157	SDN_CTRL	BVT1_AGENT	TCP	70	45376 → netconf-ssh(830)	
427	274.778774181	SDN_CTRL	BVT2_AGENT	SSHv2	134	Client: Encrypted packet	
547	360.611803332	SDN_CTRL	BVT2_AGENT	TCP	70	57140 → netconf-ssh(830)	
563	443.549071588	SDN_CTRL	BVT3_AGENT	SSHv2	134	Client: Encrypted packet	2+3
666	477.675543516	SDN_CTRL	BVT3_AGENT	TCP	70	49490 → netconf-ssh(830)	
680	478.027317244	SDN_CTRL	BVT4_AGENT	SSHv2	134	Client: Encrypted packet	
785	687.283323597	SDN_CTRL	BVT4_AGENT	TCP	70	41956 → netconf-ssh(830)	
802	687.635983212	SDN_CTRL	BVT3_AGENT	SSHv2	134	Client: Encrypted packet	4
907	712.325151216	SDN_CTRL	BVT3_AGENT	TCP	70	49494 → netconf-ssh(830)	
923	712.615324380	SDN_CTRL	BVT4_AGENT	SSHv2	134	Client: Encrypted packet	
1001	798.724533117	SDN_CTRL	BVT4_AGENT	TCP	70	41960 → netconf-ssh(830)	
1018	818.078985530	SDN_CTRL	BVT2_AGENT	SSHv2	134	Client: Encrypted packet	3
1075	902.076978897	SDN_CTRL	BVT2_AGENT	TCP	70	57164 → netconf-ssh(830)	
1092	910.307751176	SDN_CTRL	BVT4_AGENT	SSHv2	134	Client: Encrypted packet	3
1131	996.235984710	SDN_CTRL	BVT4_AGENT	TCP	70	41968 → netconf-ssh(830)	
1148	1004.133009227	SDN_CTRL	BVT1_AGENT	SSHv2	134	Client: Encrypted packet	6
1173	1009.293291528	SDN_CTRL	BVT1_AGENT	TCP	70	45414 → netconf-ssh(830)	
1190	1009.360197623	SDN_CTRL	BVT2_AGENT	SSHv2	134	Client: Encrypted packet	
1218	1010.529029640	SDN_CTRL	BVT2_AGENT	TCP	70	57178 → netconf-ssh(830)	
1234	1014.471328156	SDN_CTRL	BVT3_AGENT	SSHv2	134	Client: Encrypted packet	6
1256	1019.585805012	BVT3_AGENT	SDN_CTRL	SSHv2	278	Server: Encrypted packet	
1270	1019.603403412	SDN_CTRL	BVT4_AGENT	SSHv2	134	Client: Encrypted packet	
1301	1020.740761812	SDN_CTRL	BVT4_AGENT	TCP	70	41992 → netconf-ssh(830)	

Fig. 10. Wireshark screenshot for case 4 with relevant NETCONF messages between SDN controller and the BVT agents. Numbers represent the steps associated to each set of messages.

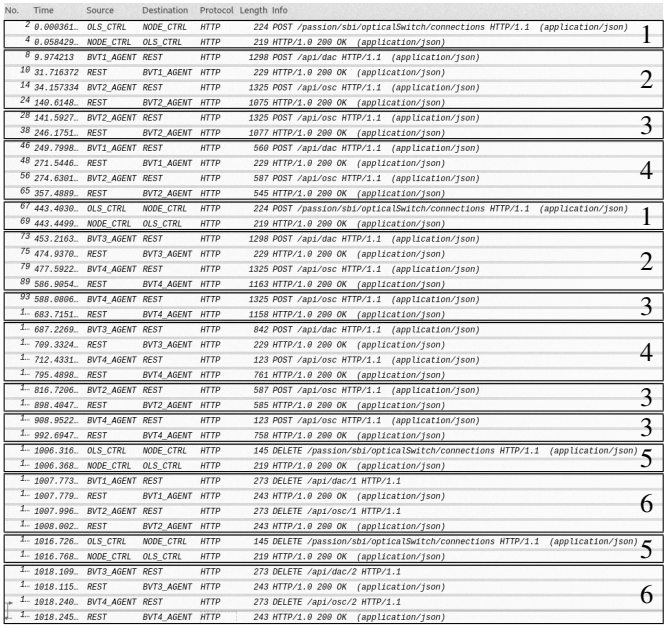

No.	Time	Source	Destination	Protocol	Length	Info	
2	0.000361…	OLS_CTRL	NODE_CTRL	HTTP	224	POST /passion/sbi/opticalSwitch/connections HTTP/1.1 (application/json)	1
4	0.058429…	NODE_CTRL	OLS_CTRL	HTTP	219	HTTP/1.0 200 OK (application/json)	
8	9.974213	BVT1_AGENT	REST	HTTP	1298	POST /api/dac HTTP/1.1 (application/json)	2
10	31.716372	REST	BVT1_AGENT	HTTP	229	HTTP/1.0 200 OK (application/json)	
14	34.157334	BVT2_AGENT	REST	HTTP	1325	POST /api/osc HTTP/1.1 (application/json)	
24	140.6148…	REST	BVT2_AGENT	HTTP	1075	HTTP/1.0 200 OK (application/json)	
28	141.5927…	BVT2_AGENT	REST	HTTP	1325	POST /api/osc HTTP/1.1 (application/json)	3
38	246.1751…	REST	BVT2_AGENT	HTTP	1077	HTTP/1.0 200 OK (application/json)	
46	249.7998…	BVT1_AGENT	REST	HTTP	560	POST /api/dac HTTP/1.1 (application/json)	4
48	271.5446…	REST	BVT1_AGENT	HTTP	229	HTTP/1.0 200 OK (application/json)	
56	274.6301…	BVT2_AGENT	REST	HTTP	587	POST /api/osc HTTP/1.1 (application/json)	
65	357.4889…	REST	BVT2_AGENT	HTTP	545	HTTP/1.0 200 OK (application/json)	
67	443.4030…	OLS_CTRL	NODE_CTRL	HTTP	224	POST /passion/sbi/opticalSwitch/connections HTTP/1.1 (application/json)	1
69	443.4499…	NODE_CTRL	OLS_CTRL	HTTP	219	HTTP/1.0 200 OK (application/json)	
73	453.2163…	BVT3_AGENT	REST	HTTP	1298	POST /api/dac HTTP/1.1 (application/json)	2
75	474.9370…	REST	BVT3_AGENT	HTTP	229	HTTP/1.0 200 OK (application/json)	
79	477.5922…	BVT4_AGENT	REST	HTTP	1325	POST /api/osc HTTP/1.1 (application/json)	
89	586.9054…	REST	BVT4_AGENT	HTTP	1163	HTTP/1.0 200 OK (application/json)	
93	588.0806…	BVT4_AGENT	REST	HTTP	1325	POST /api/osc HTTP/1.1 (application/json)	3
1…	683.7151…	REST	BVT4_AGENT	HTTP	1158	HTTP/1.0 200 OK (application/json)	
1…	687.2269…	BVT3_AGENT	REST	HTTP	842	POST /api/dac HTTP/1.1 (application/json)	4
1…	709.3324…	REST	BVT3_AGENT	HTTP	229	HTTP/1.0 200 OK (application/json)	
1…	712.4331…	BVT4_AGENT	REST	HTTP	123	POST /api/osc HTTP/1.1 (application/json)	
1…	795.4898…	REST	BVT4_AGENT	HTTP	761	HTTP/1.0 200 OK (application/json)	
1…	816.7206…	BVT2_AGENT	REST	HTTP	587	POST /api/osc HTTP/1.1 (application/json)	3
1…	898.4047…	REST	BVT2_AGENT	HTTP	585	HTTP/1.0 200 OK (application/json)	
1…	908.9522…	BVT4_AGENT	REST	HTTP	123	POST /api/osc HTTP/1.1 (application/json)	3
1…	992.6947…	REST	BVT4_AGENT	HTTP	758	HTTP/1.0 200 OK (application/json)	
1…	1006.316…	OLS_CTRL	NODE_CTRL	HTTP	145	DELETE /passion/sbi/opticalSwitch/connections HTTP/1.1 (application/json)	5
1…	1006.368…	NODE_CTRL	OLS_CTRL	HTTP	219	HTTP/1.0 200 OK (application/json)	
1…	1007.773…	BVT1_AGENT	REST	HTTP	273	DELETE /api/dac/1 HTTP/1.1	6
1…	1007.779…	REST	BVT1_AGENT	HTTP	243	HTTP/1.0 200 OK (application/json)	
1…	1007.996…	BVT2_AGENT	REST	HTTP	273	DELETE /api/osc/1 HTTP/1.1	
1…	1008.002…	REST	BVT2_AGENT	HTTP	243	HTTP/1.0 200 OK (application/json)	
1…	1016.726…	OLS_CTRL	NODE_CTRL	HTTP	145	DELETE /passion/sbi/opticalSwitch/connections HTTP/1.1 (application/json)	5
1…	1016.768…	NODE_CTRL	OLS_CTRL	HTTP	219	HTTP/1.0 200 OK (application/json)	
1…	1018.109…	BVT3_AGENT	REST	HTTP	273	DELETE /api/dac/2 HTTP/1.1	6
1…	1018.115…	REST	BVT3_AGENT	HTTP	243	HTTP/1.0 200 OK (application/json)	
1…	1018.240…	BVT4_AGENT	REST	HTTP	273	DELETE /api/osc/2 HTTP/1.1	
1…	1018.245…	REST	BVT4_AGENT	HTTP	243	HTTP/1.0 200 OK (application/json)	

Fig. 11. Wireshark screenshot for case 4. It shows the http messages exchanged between the OLS controller and the node agent; and between the BVT agents and the REST server that manages the hardware. Numbers represent the steps associated to each set of messages.

case (see Table III-A cases) and the BVT connection pair (Tx and Rx):

1) Optical channel provisioning, corresponding to actions described in sections II-B1 and II-B2.
2) Default configuration of the BVTs. This is related to actions detailed in section II-B3.
3) Monitoring of the BVT Rx performance. At this point the control loop has been started as reported in section II-B4.
4) Update of the configuration of the BVTs to optimize the performance. This is the actuator part of the action described in section II-B4.
5) Delete of the optical channel.
6) Delete of the BVTs.

This is repeated twice for each case, one time per each BVT pair. Furthermore, in order to test the performance of the BVT Rx monitoring operation, this is repeated one more time per BVT pair before deleting the optical channel and the BVTs.

Sample Wireshark screenshots are depicted in Figs. 10 and 11 for case 4. Fig. 10 shows the Wireshark screenshot with the beginning/end packages corresponding to the exchange of NETCONF messages between the SDN controller and the SDN agents. In turn, Fig. 11 depicts the Wireshark screenshot of the relevant messages between the OLS controller and node controller, and between the BVT agents and the intermediate computer hosting the DSP modules and interacting with the corresponding DACs and ADCs.

In the first step, the SDN controller configures the OLS controller, which sends the corresponding messages to the node controller in order to configure the switch matrix at the CO. This action corresponds to the messages framed as # 1 in Fig. 11. There we can observe the petition coming from the node controller and the reply message from the OLS controller.

In the second step, the SDN controller configures both BVT pairs to provision a bidirectional channel with a capacity of 22.25 Gb/s with the corresponding BVT parameters. In this initial step, regardless of the capacity demand, the same constellation is used for all the 512 subcarriers of the optical OFDM (bits per symbol = 2, and power per symbol = 1), in order to provide a fair channel estimation after step 3.

In the third step, the SDN controller requests to the BVT Rx agents the monitored SNR for the 512 subcarriers through the exchange of NETCONF messages as shown in Fig. 10. For each subcarrier, the DSP Rx performs the average of 10 ADC acquisitions of 20 μs in order to provide an accurate SNR. Please note that monitoring requests also return the BER measurement of the signals.

In Figs. 10-11 we can see the exchange of messages between all the intervening entities to configure and test the performance of the different BVTs. In fact, in the 2+3 frame of Fig. 10, we can observe the messages for configuring and monitoring both BVTs pairs. Fig. 12 shows the monitored SNR and the new values of the constellation (bits per symbol) for each subcarrier. Significant changes are observed with respect to the initial uniform loading.

After reconfiguration, step 3 is launched again in order to crosscheck the performance. In Fig. 10 we can observe the messages exchanged between the controller and the agents of BVT2 and BVT4 in order to obtain the corresponding BER and SNR. These messages trigger the communication with the REST server, shown in Fig. 11 in order to perform the data acquisition at ADC and the suitable signal processing.

Finally, in the fifth and sixth steps, the SDN controller deletes the optical channel by first removing the connection of the switching matrix (step 5) and subsequently removing the state in the BVTs (step 6). The messages for these actions are shown in Figs. 10-11. Precisely, Fig. 10 shows the the message exchange between the SDN controller and the BVT

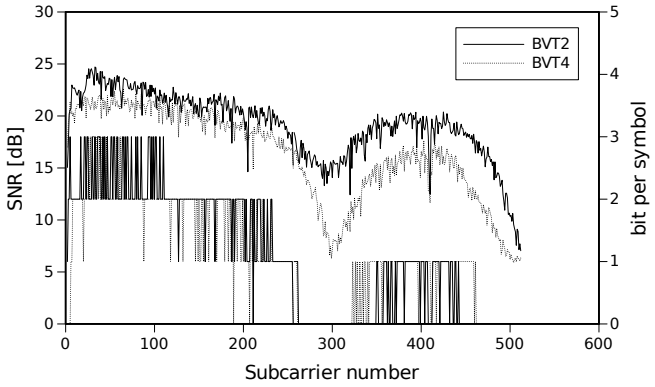

Fig. 12. Measured SNR and bit per symbol assignment for the BVTs examined.

TABLE IV
AVERAGE CONFIGURATION TIME FOR ALL THE CASES TESTED

	Time	Time exc. offline DSP
Step 1	60 ms	60 ms
Step 2+3	130 s	4 s
Step 3	90 s	4 s
Step 4	110 s	2 s
Step 5	1 s	1 s
Step 6	6 s	6 s

agents, while Fig. 11 depicts the interaction between the BVT agents and the REST server, and also the messages between the node agent and the OLS controller.

Table IV summarizes the results in terms of configuration time. There we also include the time when excluding offline signal processing according to e.g. the results shown in Fig. 11. In fact, by substracting these values to the time reported before, we can have an idea of the performance of the network in case the transceivers where working in real time. In this case, the configuration time of the different steps is 6 s or less for all the cases. Please note that steps 1, 5 and 6 do not involve offline DSP.

Tables V and VI summarize the results in terms of BER and EVM, respectively. There we can see that when using the default configuration (after step 2), performance is quite bad and does not comply with the expected values. Nevertheless, after step 4, when bit/power loading is applied, BER is more than one order of magnitude below the $2.63 \cdot 10^{-4}$ limit obtained in section II. In fact, as shown in table VI, this leads to EVM values equal to 1 % and below, being suitable for the proposed radio signals with 256QAM constellation.

TABLE V
BER OBTAINED FOR THE DIFFERENT CASES

	Case 1	Case 2	Case 3	Case 4
CO, step 2	$3.7 \cdot 10^{-2}$	$4.4 \cdot 10^{-2}$	$5.9 \cdot 10^{-2}$	$4.3 \cdot 10^{-2}$
CO, step 4	$5.1 \cdot 10^{-5}$	$1.3 \cdot 10^{-5}$	$\leq 10^{-6}$	$3.9 \cdot 10^{-5}$
RN/CS, step 2	$7.4 \cdot 10^{-3}$	$9.6 \cdot 10^{-3}$	$1.1 \cdot 10^{-2}$	$9.2 \cdot 10^{-3}$
RN/CS, step 4	$7.5 \cdot 10^{-5}$	$\leq 10^{-6}$	$1.5 \cdot 10^{-5}$	$1.3 \cdot 10^{-5}$

TABLE VI
EVM OBTAINED FOR THE DIFFERENT CASES

	Case 1	Case 2	Case 3	Case 4
CO, step 2	18.7 %	19.8 %	21.5 %	19.7 %
CO, step 4	0.9 %	0.5 %	0.1 %	0.8 %
RN/CS, step 2	10.1 %	11.2 %	11.3 %	11.0 %
RN/Cs, step 4	1.0 %	0.1 %	0.5 %	0.5 %

V. CONCLUSION

We have experimentally demonstrated a passive network able to handle up to $19 \times 40 = 760$ spatial/spectral channels. In fact, a 256-QAM 760.32 MHz radio signal, featuring a total capacity of 5.667 Gb/s has been digitized to a 22.25 Gb/s DRoF data stream and successfully transmitted over this infrastructure. At the same time, we have shown how the capacity can be set by the SDN controller by generating the suitable constellation per OFDM subcarrier after monitoring the SNR, which gives an estimation of the channel profile. This allows to optimize the transmission performance according to the required capacity. In fact, we have shown that BER can be improved by about 3 orders of magnitude with respect to uniform loading, which leads to EVM figures of 1 % and below for the reconstructed radio signal.

ACKNOWLEDGMENT

The authors would like to thank Laura Rodríguez for her effort and help building up the hardware/software interfaces.

REFERENCES

[1] M. A. Habibi, M. Nasimi, B. Han, and H. D. Schotten, "A comprehensive survey of RAN architectures toward 5G mobile communication system," *IEEE Access*, vol. 7, pp. 70 371–70 421, 2019.

[2] A. Tzanakaki, M. Anastasopoulos, N. Gomes, P. Assimakopoulos, J. M. Fàbrega, M. S. Moreolo, L. Nadal, J. Gutiérrez, V. Sark, E. Grass *et al.*, "Transport Network Architecture," *5G System Design: Architectural and Functional Considerations and Long Term Research*, 2018.

[3] S. Mikroulis, I. N. Cano, D. Hillerkuss *et al.*, "CPRI for 5G Cloud RAN? –Efficient Implementations Enabling Massive MIMO Deployment– Challenges and Perspectives," in *2018 European Conference on Optical Communication (ECOC)*. IEEE, 2018, pp. 1–3.

[4] CPRI, "Interface specification," Oct. 2015, v 7.0.

[5] H. Wang, M. A. Hossain, and C. Cavdar, "Cloud RAN architectures with optical and mm-Wave transport technologies," in *2017 19th International Conference on Transparent Optical Networks (ICTON)*. IEEE, 2017, pp. 1–4.

[6] F. Ponzini, K. Kondepu, F. Giannone, P. Castoldi, and L. Valcarenghi, "Optical access network solutions for 5G fronthaul," in *2018 20th International Conference on Transparent Optical Networks (ICTON)*. IEEE, 2018, pp. 1–5.

[7] 3GPP TS 38.211, "NR physical channels and modulation," Mar. 2019, 3GPP Rel. 15.

[8] L. Zhang, A. Udalcovs, R. Lin, O. Ozolins, X. Pang, L. Gan, R. Schatz, M. Tang, S. Fu, D. Liu, W. Tong, S. Popov, G. Jacobsen, W. Hu, S. Xiao, and J. Chen, "Toward Terabit Digital Radio over Fiber Systems: Architecture and Key Technologies," *IEEE Communications Magazine*, vol. 57, no. 4, pp. 131–137, April 2019.

[9] S. Rommel, D. Perez-Galacho, J. M. Fabrega, R. Muñoz, S. Sales, and I. Tafur Monroy, "High-Capacity 5G Fronthaul Networks Based on Optical Space Division Multiplexing," *IEEE Transactions on Broadcasting*, vol. 65, no. 2, pp. 434–443, June 2019.

[10] J. M. Fabrega, R. Muñoz, M. S. Moreolo, L. Nadal, M. Eiselt, F. Azendorf, J. P. Turkiewicz, P. W. L. van Dijk, S. Rommel, and I. T. Monroy, "Digitized Radio-over-Fiber Transceivers for SDM/WDM Back-/Front-Haul," in *2019 21st International Conference on Transparent Optical Networks (ICTON)*, July 2019, pp. 1–4.

[11] J. M. Rivas-Moscoso, B. Shariati, A. Mastropaolo, D. Klonidis, and I. Tomkos, "Cost benefit quantification of sdm network implementations based on spatially integrated network elements," in *ECOC 2016; 42nd European Conference on Optical Communication*, Sep. 2016, pp. 1–3.

[12] R. Munoz, N. Yoshikane, R. Vilalta, J. M. Fabrega, L. Rodriguez, D. Soma, S. Beppu, S. Sumita, R. Casellas, R. Martinez, T. Tsuritani, and I. Morita, "Adaptive software defined networking control of space division multiplexing super-channels exploiting the spatial-mode dimension," *IEEE/OSA Journal of Optical Communications and Networking*, vol. 12, no. 1, pp. A58–A69, January 2020.

[13] E. Riccardi, P. Gunning, O. G. de Dios, M. Quagliotti, V. López, and A. Lord, "An Operator view on the Introduction of White Boxes into Optical Networks," *J. Lightw. Technol.*, vol. 36, no. 15, pp. 3062–3072, Aug 2018.

[14] 3GPP TS 38.801, "Study on new radio access technology: Radio access architecture and interfaces," Mar. 2017, 3GPP Rel. 14.

[15] N. Sambo, P. Castoldi, A. D'Errico, E. Riccardi, A. Pagano, M. S. Moreolo, J. M. Fabrega, D. Rafique, A. Napoli, S. Frigerio, E. H. Salas, G. Zervas, M. Nolle, J. K. Fischer, A. Lord, and J. P. F. P. Giménez, "Next generation sliceable bandwidth variable transponders," *IEEE Commun. Mag.*, vol. 53, no. 2, pp. 163–171, Feb. 2015.

[16] J. M. Fabrega, M. Svaluto Moreolo, L. Nadal Reixats, F. J. Vílchez, R. Casellas, R. Vilalta, R. Martínez, R. Muñoz, J. P. Fernández-Palacios, and L. M. Contreras, "Experimental validation of a converged metro architecture for transparent mobile front-/back-haul traffic delivery using SDN-enabled sliceable bitrate variable transceivers," *J. Lightw. Technol.*, vol. 36, no. 7, pp. 1429–1434, Apr. 2018.

[17] M. Svaluto Moreolo, J. M. Fabrega, L. Nadal, F. J. Vílchez, A. Mayoral, R. Vilalta, R. M. noz, R. Casellas, R. Martínez, M. Nishihara, T. Tanaka, T. Takahara, J. C. Rasmussen, C. Kottke, M. Schlosser, R. Freund, F. Meng, S. Yan, G. Zervas, D. Simeonidou, Y. Yoshida, and K.-I. Kitayama, "SDN-enabled sliceable BVT based on multicarrier technology for multiflow rate/distance and grid adaptation," *J. Lightw. Technol.*, vol. 34, no. 6, pp. 1516–1522, Mar. 2016.

[18] R. Muñoz *et al.*, "Autonomic SDN Control of Multi-Adaptive OFDM-Based BVTs in Partially-Disaggregated SDM/WDM Fronthaul Networks," in *2019 European conference on optical communications (ECOC)*, Sept. 2019, pp. 1–4.

[19] R. Muñoz, J. Fàbrega, R. Vilalta, M. S. Moreolo, R. Martínez, R. Casellas, N. Yoshikane, T. Tsuritani, and I. Morita, "SDN control and monitoring of SDM/WDM and packet transport networks for 5G fronthaul/backhaul," in *2018 IEEE Photonics Society Summer Topical Meeting Series (SUM)*. IEEE, 2018, pp. 151–152.

[20] R. Muñoz, N. Yoshikane, R. Vilalta, J. M. Fàbrega, L. Rodríguez, R. Casellas, M. S. Moreolo, R. Martínez, L. Nadal, D. Soma, Y. Wakayama, S. Beppu, S. Sumita, T. Tsuritani, and I. Morita, "SDN Control of Sliceable Multidimensional (Spectral and Spatial) Transceivers with YANG/NETCONF," *J. Opt. Commun. Netw.*, vol. 11, no. 2, pp. A123–A133, Feb 2019. [Online]. Available: http://jocn.osa.org/abstract.cfm?URI=jocn-11-2-A123

[21] L. Nadal, M. S. Moreolo, J. M. Fàbrega, A. Dochhan, H. Grießer, M. Eiselt, and J.-P. Elbers, "DMT modulation with adaptive loading for high bit rate transmission over directly detected optical channels," *J. Lightw. Technol.*, vol. 32, no. 21, pp. 3541–3551, Nov 2014.

[22] R. Muñoz, J. M. Fabrega, R. Vilalta, L. Rodríguez, L. Nadal, R. Casellas, and R. Martínez, "Autonomic sdn control of multi-adaptive ofdm-based bvts in fully-disaggregated sdm/wdm fronthaul networks," in *45th European Conference on Optical Communication (ECOC 2019)*. IET, 2019, pp. 1–4.

[23] "CTTC ONS github repository for BVT yang model," 2019. [Online]. Available: https://github.com/CTTC-ONS/BVT/tree/master/YANG

[24] R. Casellas, F. J. Vílchez, L. Rodríguez, R. Vilalta, J. M. Fàbrega, R. Martínez, L. Nadal, M. S. Moreolo, and R. Muñoz, "An ols controller for hybrid fixed/flexi grid disaggregated networks with open interfaces," in *2020 Optical Fiber Communications Conference and Exhibition (OFC)*. IEEE, 2020, pp. 1–3.

[25] "ONF technical recommendation. Functional Requirements for Transport API," *ONF TR-527*, 2016.

[26] "An extensible YANG validator and converter in Python," 2019. [Online]. Available: https://github.com/mbj4668/pyang

[27] "A plugin for pyang that creates Python bindings for a YANG model," 2019. [Online]. Available: https://github.com/robshakir/pyangbind